5 FC 12 00



Proceedings of the International Symposium on Laser Metrology for Precision Measurement and Inspection in Industry

Florianópolis, Brazil October 13-15, 1999

edited by Armando Albertazzi Jr.

## Promoted by:



The International Measurement Confederation
Technical Committee on Measurement of Geometrical
Quantities – TC 14
Laser Measurement Working Group of

METRO!

The Brazilian Society of Metrology



The International Society for Optical Engineering

#### Editor:

Prof. Dr. Armando Albertazzi Jr

Federal University of Santa Catarina Mechanical Engineering Department LABMETRO – Metrology and Automation Laboratory Florianópolis, SC – Brazil albertazzi@labmetro.ufsc.br

Laser Metrology 1999
Proceedings of the International Symposium on
Laser Metrology for Precision Measurement and
Inspection in Industry,
held in Florianópolis, Brazil, 13-15 October, 1999
Ed. by Armando Albertazzi Jr.

### © International Measurement Confederation - IMEKO

All rights reserved. No part of this book may be reproduced in any form without written the permission from the IMEKO. Registered names, trademarks, etc, used in this book, even when not specifical market as such, are not to be considered unprotected by law.

Printed in Brazil



# preface

Since the laser was made commercially available in early 60's, people from diverse areas started to develop very different applications for it. Laser has been particularly attractive for measurement and inspection tasks, since it provides a very fast way to acquire precisely quantitative information from a measurand without any physical contact. Nowadays, laser metrology is a very rich and growing subject, widely used in science and industry. Applications ranging from nanometrology to large-scale 3D measurement has been successfully applied in different fields.

This volume contains the papers presented during the International Symposium on Laser Metrology for Precision Measurement and Inspection in Industry, held in Florianópolis, October 13-15, 1999. This is a "first time" event in many aspects: the first time that an IMEKO event is held in South America, the first time that the SPIE runs an event in cooperation with IMEKO, and again the first time that a SPIE event is held in South America and, of course, the first time that an event is organized in cooperation among IMEKO, SPIE and the Brazilian Society for Metrology.

Contributions from 54 papers from all over the world bring a very diversified sample of what has been developed and used worldwide for measurement and inspections tasks. This rich material is here organized in five modules:

Module 1 deals with **length, shape and position measurement**. Precision measurement of high quality cylinders, geometrical testing of machines and measurement systems, absolute distance measurement, 3D shape measurement and precision measurement of gage blocks lengths are examples of what can be found in this module.

Module 2 is dedicated to **in process measurement and testing**. Most of papers deal with applications very closely related to manufacturing processes. Several industrial applications of range finders, from vision systems for AGV to control the unloading of railway wagons, are included. Other applications involve thin film thickness measurement in the spinning process, weld and machine tool testing and corrosion monitoring.

Module 3 is devoted to sensors, new instruments and performance evaluation. Recent advances in several areas are reported, as, for example, the basis of a new generation of lasermikes as well as strategic challenges in laser metrology, are presented. An atomic clock optically operated is also presented. Evaluations of optoelectronic components, sensors and laser light properties are also included plus a very useful user guide for IR sensors is included as a keynote paper.

Module 4 is titled **holography**, **speckle metrology and interferometry**. Several papers are dealing with ESPI (electronic speckle pattern interferometry), ranging from fringe processing techniques to several specific applications: simultaneous shape and deformation measurement, endoscopic measurement, residual stresses measurement, material properties measurement, dynamic measurements and a robust ESPI measurement technique. Additional interferometric techniques and applications are also presented.

Finally, module 5 is concerned with **microgeometry and nanotechnology**. This module includes a keynote paper on characterization of engineered surfaces. Laser based measurement systems and techniques for microgeometry characterization are reported. Specific systems, techniques and applications of roughness measurements are also included.

#### ACKNOWLEDGEMENTS

Matthias Chour has gained much from discussions with many, including Bernhard Hils, Wolfgang Heinze. Salvatore Donati and Samuel Lévêque.

#### REFERENCES

- [1] Schneider, C.A.; Pfeiffer, G.: Metrological Support to Small and Medium-sized Industries. In: E.Seiler (ed): Proceedings of the IMEKO TC 11 Symposium "The Role of Metrology in Economicand Social Development" Braunschweig, June 16-19, 1998 Germany. PTP-Texte band 9 pp361-373. Braunschweig: Physikalisch-Technische Bundesanstalt 1998
- [2] Pfeifer, T.; Imkamp, D.: Optimization Potential in Manufactoring Metrology. In: O. Aumala (ed): New measurements-Challenges and Visions. Proceedings of the XIV IMEKO World Congress Tampere, Finnland. Topic 14. CD-ROM ISBN 951-96042-9-4. Helsinki:IMEKO-SAS 1997
- [3] Hofmann,D.: New opto-electronic measuring instruments for precision equipment and other machinery. In: K.Ono (ed): Proceeding of the International Conference on Micromechatronics for Information and Precision Equipment MIPE'97. Pp.171-174. Tokyo: The japan Society for mechanical Engineering 1997
- [4] Hofmann,D.; Machalett, E.; Kokott,J.; Müller,D.: Visualisation of multifunctional intelligent PC measurements for inplant quality control. In: K. Kariya (ed). Artificial Intelligence Based measurement and Control AIMaC '91. Proceedings of the 8<sup>th</sup> IMEKO TC7 Symposium1991. Kyoto: Ritsumeikan University 1991
- [5] Müller, J.; Chour, M.: Two-frequency laser interferometric path measuring system for extreme velocities and high accuracy's. International Journal of Optoelectronics 8(1993)5/6, 647-654
- [6] Lévêque,S.: Méthodes et systèmes Laser pour l'analyse du trajet optique interne du très grand télescope interferometrique européen, VLTI. These. Présentée pour obtenir le titre de Docteur de L'Universite Louis Pasteur de Strasbourg
- [7] Grüner.E.: Vermessung von Brückenbogen. internal CZO 1994

# Fabrication of hybrid diffractive and refractive optical element for multiple line generation over high angle

Luiz Gonçalves Neto", Luciana Brassolatti Roberto", Patrick Verdonck<sup>b</sup>, Ronaldo Domingues Mansano<sup>b</sup>, Giuseppe Antonio Cirino<sup>b</sup> and Mario Antonio Stefani<sup>c</sup>

"EESC - University of São Paulo, São Carlos - SP, Brasil, lgneto@sel.eesc.sc.usp.br

bLSI - EPUSP - University of São Paulo - São Paulo - SP - Brazil, mansano@lsi.usp.br

"Opto Eletrônica S/A, São Carlos - SP, Brasil, stefani@opto.com.br

ywords: Multiple line generation over high angle, hybrid diffractive and refractive optical element, diffractive optical ment.

#### ABSTRACT

A hybrid diffractive and refractive optical phase element capable of splitting a monochromatic laser beam into an itrary number of lines over high angle is presented. The element is formed by a binary surface-relief computer generated ise hologram and a continuous parabolic surface-relief phase grating acting as an array of divergent parabolic lenses. The ary surface-relief was generated into one side of a quartz substrate and the parabolic profile was generated into a thick photo ist deposited in the other side of the quartz substrate. It was calculated that a divergent parabolic lens with f-number of 0.5 uld deliver the desired optical pattern of multiple beams distributed over 90°. A surface relief depth of 6.5 µm was rulated considering the phase distributions of such lens. The parabolic profile were fabricated in a 10 µm thick photo ist, using a contact printer exposure through a mask with a repetitive 4 µm line - 6 µm space pattern. The developer reentration and development time were fixed for these tests and the exposure time was varied in order to obtain the desired file. The resulting diffraction patterns were characterised and a satisfying result was obtained. This pattern can be used in ot vision and other applications.

#### 1. INTRODUCTION

The split of a laser beam into an arbitrary number of lines over high angle is required for several industrial plications like movement detection and robot vision. The line intensity distribution has to be uniform and it is desired to re a high diffraction efficiency in the process.

Computer generated phase holograms are well known devices for beam shaping 14. An arbitrary distribution of lines in high diffraction efficiency could be obtained in the reconstruction plan using those holograms. As they are calculated sed on the scalar diffraction, the smallest hologram structure must be several times larger than the wavelength, limiting the e of the reconstructed image distribution in the reconstruction plan, and consequently limiting the fan-out angle.

A line distribution over high angle could be generated using a low f-number (f < 0.5) cylindrical lens. The limitation hat only one line can be generated using this approach. Also, it is not common that the diameter of a lens is greater than focal length, i.e., the f-number of a lens is almost always greater than 1. A f/1 lens is a very expensive and highly rected lens.

A line distribution over a high angle could be generated using an array of dielectric cylinders or parabolic sections ing as an array of convergent or divergent low f-number cylindrical lenses. Many authors have reported the diffraction perties of a continuous conical phase relief grating for uniform multiple beam splitting  $^{8,10,11}$ . In those gratings, all the light concentrated just behind the grating, producing an array of light point sources that can be represented by the light ensity distribution I(u)=comb(u/U). The Fraunhofer diffraction pattern of the grating is obtained by the Fourier transform of ), giving I(x)=Ucomb(Ux). Here again, the limitation is that only one non-continuous line can be generated using this proach.

In this work we present a hybrid diffractive phase element capable to split a laser beam into an arbitrary number of es over 90°. The element is formed by a binary surface-relief computer generated phase hologram and a continuous abolic surface-relief phase grating, as shown in figure 1b. The binary surface-relief computer generated phase hologram is do generate an arbitrary number of lines and the parabolic surface-relief phase grating is used to split the laser beam over igh angle. This parabolic surface-relief phase grating acts as an array of divergent cylindrical lenses. The binary surface-relief was generated into one side of a quartz substrate and the parabolic profile was generated into a thick photo resist posited in the other side of the quartz substrate.

250300



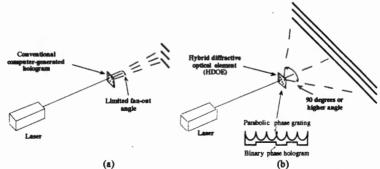


Figure 1: (a) Conventional computer generated phase holograms calculated based on scalar diffraction have limited fan-out angle. (b) Hybrid diffractive optical phase elements are capable to split of a perpendicular laser beam into an arbitrary number of lines over high angle.

#### 2. PRINCIPLE OF THE HYBRID DIFFRACTIVE AND REFRACTIVE OPTICAL PHASE ELEMENT

The sampling function  $G_v(u,v)$  which describes a regular phase hologram consists of a finite array of rectangular pixels of width  $U^*$  and  $V^*$ . The pixels center are spaced at regular intervals of width U in the u direction and regular intervals of width v in the v direction, with  $v^* \le v$  and  $v^* \le v$ , as illustrated in figure 2. Considering the sampling theorem, the hologram structure is represented by

$$G_{s}(u,v) = \left\{ \left[ rect \left( \frac{u}{U^{*}} \right) rect \left( \frac{v}{V^{*}} \right) \right] \bullet \left[ comb \left( \frac{u}{U} \right) comb \left( \frac{v}{V} \right) G(u,v) \right] \right\} \left[ rect \left( \frac{u}{NU} \right) rect \left( \frac{v}{MV} \right) \right]$$

$$\tag{1}$$

where G(u,v) is the ideal continuous phase distribution of the hologram, N is the number of pixels in the u direction, M is the number o pixels in the v direction, and  $\otimes$  indicates a two-dimensional convolution. The reconstruction  $g_v(x,y)$  is obtained performing the Fourier Transform of  $G_v(u,v)$ :

$$g_{x}(x,y) = NMU^{2}V^{2}U^{*}V^{*}\left\{\left[\operatorname{sinc}\left(U^{*}x\right)\operatorname{sinc}\left(V^{*}y\right)\right]\left\{\left[\operatorname{comb}\left(Ux\right)\operatorname{comb}\left(Vy\right)\right] \bullet g(x,y)\right\}\right\}$$

$$\bullet\left[\operatorname{sinc}\left(NUx\right)\operatorname{sinc}\left(MVy\right)\right] \tag{2}$$

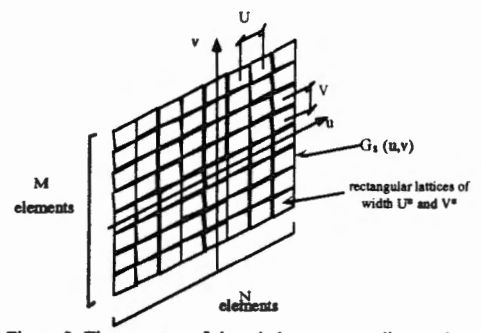


Figure 2: The structure of phase holograms usually consists of a finite array of rectangular pixels of width  $U^*$  and  $V^*$ , with centers spaced at regular intervals of width U in the u direction and V in the v direction, with  $U^* \subseteq U$  and  $V^* \subseteq V$ .

where g(x,y) is the reconstruction of the ideal continuous hologram G(u,y). In equation 2, the term sinc(NUx)sinc(MvUy) at right is the contribution due to the finite hologram's extension NUxMV, and the term sinc(U\*x)sinc(V\*v) at left is due to the finite dimension U\*xV\* of each hologram's pixel. The reconstruction g(x,y) can be obtained by performing the convolution of the factor sinc(NUx)sinc(MVy), with the result obtained by the multiplication between the attenuation factor sinc(U\*x)sinc(V\*y) and the replication of the reconstruction of g(x,y) at each point (n/U, m/V) of the comb function in the (x,y) plane, with  $-\infty \le n, m \le +\infty$ .

If the ideal hologram phase distribution G(u,v) is not limited over a finite extension NUxMV in the (u,v) plane, only a partial phase information of G(u,v) will be stored in the sampled hologram G<sub>2</sub>(u,v). Consequently, the convolution of

the term sinc(NUx)sinc(MVy) can causes a speckle noise pattern 13,14 over the reconstruction g<sub>1</sub>(x,y).

Analyzing again the first part of equation 2 we verify that when the term sinc(U\*x)sinc(V\*y) is not present, which means that the sampling function is only the array of delta functions comb(u/U)comb(v/V), the reconstruction g(x,y) will be replicated at each point (n/U, m/V), where n and m are integers in the (x,y) plane, with  $\infty \le n, m \le +\infty$ . If the reconstruction g(x,y) generates horizontal parallel lines over a region (1/U)x(1/V) centered in the reconstruction plane, as shown in figure 1a, the replication of g(x,y) in the x direction will achieves the condition of splitting a laser beam into an arbitrary number of lines over high angle as shown in figure 1b.

To eliminate the undesirable replication of the reconstruction g(x,y) in the y direction, a new sampling function

should be considered. This new sampling function is shown in the equation 3:

$$G_{\mathbf{s}}^{\mathbf{d}}(u,v) = \left\{ \delta(u) \operatorname{rect}\left(\frac{v}{V}\right) \right\} \otimes \left[ \operatorname{comb}\left(\frac{u}{U}\right) \operatorname{comb}\left(\frac{v}{V}\right) G(u,v) \right] \right\} \left[ \operatorname{rect}\left(\frac{u}{NU}\right) \operatorname{rect}\left(\frac{v}{MV}\right) \right] \tag{3}$$

Now, the sampling function Gi (u,v) consists of an array of delta functions spaced at regular intervals of width U in the u direction and rectangular functions of width V spaced at regular intervals of width V in the v direction. Performing the Fourier transform of G'(u,v) we have the new reconstruction g'(x,v)

$$g_{*}^{sl}(x,y) = NMU^{2}V^{3}\left\{\operatorname{sinc}(Vy)\left\{\left[\operatorname{comb}(Ux)\operatorname{comb}(Vy)\right]\otimes g(x,y)\right\}\right\}\otimes\left[\operatorname{sinc}(NUx)\operatorname{sinc}(MVy)\right]$$
(4)

From equation 4 we verify that the factor sinc(Vy) causes a attenuation in the replication of the reconstruction g(x,y) at each point (m/V),  $-\infty \le m \le +\infty$ , in the y direction. The replication of g(x,y) in the x direction is not attenuated, achieving the

diffraction condition of high angle splitting in the x direction as shown in figure 1b.

This behavior could be approximated by decreasing pixel's size U\*, or by sampling the function G(u,v) using a function that partially reproduces a light point source in the u direction. Due to the reduction of the diffraction efficiency, it is not of interest to minimize the pixel's size U\*. Also, considering the difficulties in the fabrication of such device, it is very complicated to reproduce the behavior of a delta function making each pixel acts as low f-number cylindrical lens, producing light point sources in the u direction just behind the each pixel.

To solve this problem we present a hybrid diffractive and refractive optical phase element formed in one side by the sampled phase hologram G<sub>t</sub>(u,v), and in the other side by a continuous parabolic surface-relief phase grating acting as an array of divergent cylindrical lenses of width UxMV in the u direction, as shown in figure 5. Equation 5 describes the sampling function of the resulted hybrid diffractive phase element Gh(u,v):

 $G_s^b(u,v) = G_s(u,v)$ .  $\left\{ \exp \left( \frac{i}{2} \frac{v}{u^2} \right) \operatorname{rect} \left( \frac{u}{U} \right) \operatorname{rect} \left( \frac{v}{MV} \right) \right\} \otimes \operatorname{comb} \left( \frac{u}{U} \right) \right\}$ (5)

where and f is the focal length of the divergent cylindrical lenses in the grating array. Neglecting the term rect(v/MV) and performing the Fourier Transform of equation 5 we have  $g^h(x,y)$ 

$$g_s^h(x,y) = g_s(x,y) \otimes \left\{ U^2 \left[ \sqrt{\lambda f} \exp(-j\pi \lambda f x^2) \otimes \text{sinc}(Ux) \right], \text{comb}(Ux) \right\}$$
 (6)

From equation 6 we verify that decreasing the focal length f, making all the light to be concentrated just behind 12 the lens, the term (-jπλfx2) vanishes, resulting in the desired condition

$$g_{*}^{h}(x,y) = S_{f} g_{*}(x,y) \otimes \{comb(Ux)\}$$
 (7)

where S<sub>f</sub> is a scaling factor.

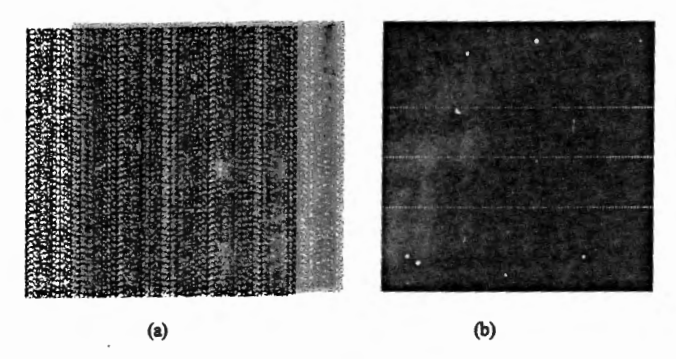


Figure 3: (a) 256x256 binary hologram. The black pixels represents the phase value  $\exp(-j\pi)$  and the white pixels the phase value  $\exp(-j0)$ ; (b) the hologram's computer reconstruction.

#### 3. THE ELEMENT DESIGN AND FABRICATION

The binary computer generated phase hologram which is present in the hybrid diffractive and refractive opt element was designed applying the iterative algorithm. The hologram distribution  $G_{kl}$  was calculated to generate the parallel lines in the reconstruction plane as shown in figure 1a and 3b. A hologram space bandwidth product (SBP) 256x256 pixels was used in the calculus. Figure 3a shows the hologram and figure 3b the computer hologram reconstruction. In figure 3a, the black pixels represents the phase value  $\exp(-j\pi)$  and the white pixels the phase value  $\exp(-j\pi)$  for resulted hologram was repeated four times in the vertical direction and four times in horizontal direction, resulting in final hologram of 1024x1024 pixels. This reduces the speckle noise pattern. Over the reconstruction caused by the rando phase used in the iterative algorithm.

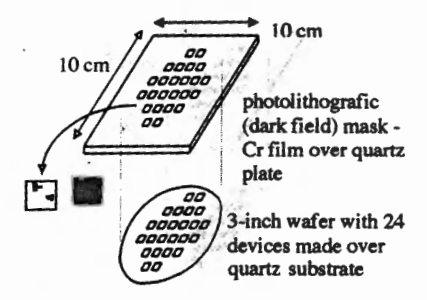


Figure 4: Conceptual design of the lithographic mask and pattern transfer to the wafer.

The final "0" and " $\pi$ " hologram's phase distribution was used to fabricate a lithography binary mask. Each mask consists of 24 of these devices as shown in figure 4. Considering the work wavelength of 0.6328  $\mu$ m, the mask's pixels size was fabricated to have the dimension of 10x10 micrometer, which respect the limits imposed by the scalar diffraction. The hologram was generated into a quartz substrate using a standard lithography process. A 1.5 micrometer thick Tokyo Ohka resist was patterned onto a 3 inch quartz wafer using the binary mask. Then the wafer was etched in a home built plasma etching system <sup>16</sup>. A mixture of CF4 end H2 gases was used <sup>17</sup>. The pressure was 150 mTorr and 150 W of power was applied to the 6 inch diameter lower electrode (in Reactive Ion Etching mode). This results in a quartz etch rate of approximately 55 nm/min and a resist etch rate of approximately 55 nm/min and a resist etch rate of approximately 65 nm/min. The total etching time depends on the desired

step height, which depends on the wavelength of the laser.

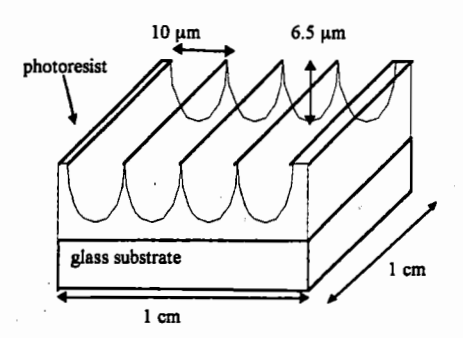


Figure 5: Schematic view of the desired parabolic surface-relief phase grating acting as an array of divergent cylindrical lenses.

To obtain a diffraction angle of 90°, each virtual lens focal plane of the a continuous parabolic surface relief phase grating has to be located at a distance of half width of the lens diameter, what results in a f-number of 0.5. Because of the used equipment, the resist thickness has to be in the 5  $\mu$ m to 10  $\mu$ m range. The width of the lens was chosen to be 10  $\mu$ m, resulting in focal distance of 6.5  $\mu$ m. It is possible to calculate the form of the ideal lens and for this application, a divergent parabolic lens was found to be a good solution. The dimensions of the parabola were designed considering that each surface acts as a divergent cylindrical lens with a f-number equal to 0.5. A surface relief depth of 6.5  $\mu$ m was calculated considering the phase distributions of such lens<sup>7</sup>, the wavelength used (0.6328  $\mu$ m) and the index of refraction of the photo resist. A schematic view of the desired surface relief is shown in figure 5.

The typical resist thickness for microelectronic applications is 1  $\mu$ m. In order to deposit a layer of at least 6.5  $\mu$ m, a special resist was used: the All-Resist AR-P320. This resist was spun on the other side of the 3-inch diameter quartz wafer with the binary holograms, during 10 seconds at 2000 rpm, after which the spin speed was accelerated up to 4000 rpm where it remained for an extra 25 seconds. This results in a layer of approximately 10  $\mu$ m thick.

In order to understand the obtained results, it is necessary to explain briefly the mechanism of diffraction through a mask with relatively small line-space features<sup>18</sup> used to generate the parabolic relief depth. The effect of light diffraction is shown in figure 6. The modulation of the light behind the mask is less than 1: light penetrates under the metal line on the mask and its intensity is not constant under the open space.

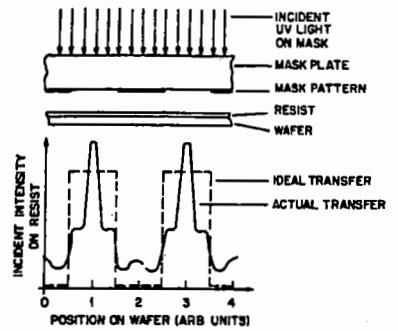


Figure 6: Ideal and real intensity distribution of light passing through a mask with narrow spaces 18.

The smaller the open space, the larger the diffraction effects. For a contact printer, the diffraction effect is larger when the distance between wafer and mask is bigger. This also means that for a thick resist, there is more diffraction than for a thir resist. In this application, diffraction is used to our advantage: in order to obtain the desired parabolic profile, we want the light to penetrate under the mask and to have a non-uniform light intensity in the open space. For all these reasons, the mask design consists of one thousand twenty four  $10240 \mu m \log 4 \mu m$  wide lines, with spaces of 6  $\mu m$  between them (the finabinary hologram is  $10240 \times 10240 \mu m$  wide). Each mask consists of 24 of these devices, spaced at the same distance used for the fabrication of the binary holograms, as shown in figure 7.

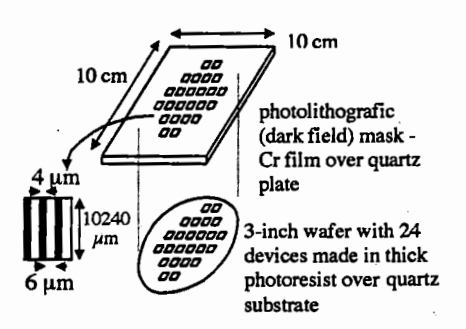


Figure 7: Conceptual design of the lithographic mask and pattern transfer to criate a continuous parabolic surface relief phase grating.

In standard microelectronic applications, the walls of the resulting resist patterns have to be as vertical as possible. In this application, the desired profile is completely different. The three most important parameters to be optimised in the lithography process are: exposure time, developer concentration and development time. A higher developer concentration results in steeper resist walls, which is preferable for microelectronic applications but not for this application. Whereas for microelectronic applications a 4:3 DI-water developer mixture was used, a mixture of 5:2 was used for this application. Several tests were performed and a development time of 1 minute was found to yield good results. The exposure times were varied from 34 to 40 seconds and the resulting resist profiles were analysed. The resulting profiles on top of a silicon wafer are shown in the SEM micrographs of figure 8. The final hybrid diffractive optical element is shown in Figure 9.

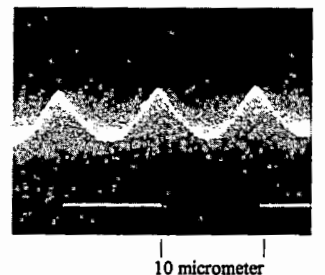


Figure 8: SEM micrograph of the resulting resist profile on top of a quartz wafer

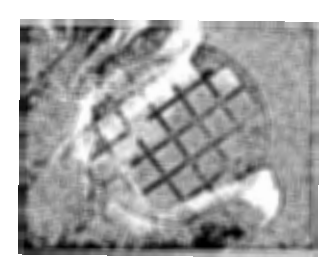


Figure 9: Hybrid diffractive optical phase element capable of splitting a laser beam into an arbitrary number of lines over high angle.

#### 4. CONCLUSIONS

A hybrid diffractive optical phase element capable of splitting a laser beam into an arbitrary number of lines over high angle has been designed and manufactured. A continuous parabolic surface relief phase grating has been fabricated in a 10 µm thick photo resist. This parabolic surface-relief phase grating acts as an array of divergent cylindrical lenses. The 10 µm wide and 6.5 µm deep approximately parabolic profiles were obtained by varying the exposure time of a contact printing process. Preliminar optical characterization shows that a laser beam can be deflected over an angle of more than 90°. Experimental results will be shown during the presentation. This work is supported by FAPESP, CNPq, CAPES and Opto-Eletrônica S.A..

#### REFERENCES

- H. Dammann and K. Görtler, "High-efficiency in-line multiple imaging by means of multiple phase holograms", Opt. Comum. 3, 312-315 (1971).
- A. Vasara, M. R. Taghizadeh, J. Turunen, j. Westerholm, E. Noponen, H. Ichikawa, J. M. Miller, T. Jaakkola, and S. Kuisma, "Binary surface-relief gratings for array illumination in digital optics", Applied Optics, Vol. 31, No. 17, pp.3320-3336, (1992).
- 3. C. Zhou and L. Liu, "Numerical study of dammann array illuminators", Applied Optics, Vol. 34, No. 26, pp. 5961-5969, (1995).
- 4. R.W. Gerchberg and W.O. Saxton. "A Practical Algorithm for the Determination of Phase from image and Diffraction Plane Pictures", Optick 35, 237-46, 1972.

  5. J.R. Fienup. "Iterative method applied to image reconstruction and computer-generated holograms". Optical
- Engineering, vol. 19 no.3, p.297-305, June 1980.
- 6. Frank Wyrowski. "Diffractive optical elements: iterative calculation of quantized, blase phase structures". Journal of Optical Society of America A, vol.7 No.6, p.961-969, june 1990.
- J. W. Goodman, "Introduction to Fourier Optics Second Edition", pp.351, McGraw-Hill, (1996).
- D. C. O'Shea, "Elements of Modern Optical Design", pp. 76, John Wiley & Sons, Inc, (1985).
- P. Langois and R. Beaulieu, "Phase relief gratings with conic section profile used in the production of multiple beams", Applied Optics, Vol. 29, No. 23, pp. 3434-3439, (1990).
- 10. R. Magnusson and D. Shin, "Diffraction by periodic arrays of dielectric cylinders", J. Opt. Soc. Am. A, Vol. 6, No. 3, pp. 412-414, (1989).
- 11. I. Aubrecht and M. Miler, "Profile of relief phase gratings used for uniform multiple beam spliting", Optics Letters, Vol. 18, No. 6, pp.1287-1289, (1993).
- 12. H. Machida, J. Nitta, A. Seko, and H. Kobayashi, "High-efficiency fiber grating for producing multiple beams of uniform intensity", Applied Optics, Vol.23, No. 2, 15 Jnuary 1984, pp. 330-332.
- 13. F. Wyrowski and O. Bryngdahl, "Speckle-free reconstruction in digital holography", JOSA A, Vol.6(8), pp. 1171-1174, Augut 1989.